ATLAS Internal Note
TILECAL-NO-026
3 October 1994

Estimation of the magnetic field in PM-cavities and tiles of the ATLAS tile-calorimeter

F. Bergsman
PPE-EC

1. Introduction

There was not enough computing power available to include the complete tile calorimeter in a model to determine the magnetic field of the Atlas detector. Here the tiles were treated as a homogeneous anisotropic material.

If one defines $\overline{B} = \int_{tile} B dv / V_{tile}$ and $\overline{H} = \int_{tile} H dv / V_{tile}$, with Vtile the volume of the smallest block from which the full tile structure can be build, one has

$$\mathrm{div}\, B = 0 \rightarrow \mathrm{div}\, \overline{B} = 0 \quad \mathrm{rot}\, H = J \rightarrow \mathrm{rot}\, \overline{H} = \overline{J}$$

and B can be replaced by $\overline{B}$, H by $\overline{H}$ in a model of the full detector to calculate the magnetic field, without using the tile structure in detail.

The relation between $\overline{B}$ and $\overline{H}$ is calculated on a small test cell with complete tile structure.

This method implies that the rate of change of the averaged field is small over the tile dimension.

The FEM-program TOSCA from Vector Fields Ltd. Oxford UK was used.

2. BH-curves

The dimensions of the test-cell were: scintillators 100 x 4 mm^2, iron sheets 104 x 4 mm^2 and iron plates 5 mm thick.

A typical field configuration is given in fig.1 .

The axes will be called: dir1 = tile direction (largest dimension of scintillator), dir2 = inside plane formed by metal plates and perpendicular to dir1, dir3 = perpendicular to metal plates.

For dir1 one expects, since (volume Fe)/(total volume) = .782, a $\overline{BH}$ curve with

$$M_1(H) = .782 \times M_{Fe}(H) \qquad (1)$$

in which $M = B / \mu 0 - H$.

In fig.2 the calculated $\overline{BH}$ curve for dir2 is given (=O). This curve can be very well approximated by

$$M_2(H) = .76 \times M_{Fe}(H) \qquad (2)$$

The BH-curve of Fe is printed with triangles in fig. 2. If the tiles would be aligned (and 4 mm broader), a laminated structure would result with

$$M_{2l}(H) = .782\ (=14/18) \times M_{Fe}(H) \qquad (3)$$

One sees that the difference between (1), (2) and (3) is small.

In fig. 3 the $\overline{BH}$ curve for dir3 is given (=O). Also this curve can be reproduced by scaling the Fe BH-curve:

$$M_3(H) = .068 \times M_{Fe}(H) \qquad (4)$$

Due to the non-linear dependence of μ on H, the $\overline{BH}$-curve in one direction will change if an H-field is applied in one of the other two directions. In fig. 2 the $\overline{BH}$ curve in dir2 is given with a field of 200 Am in dir3 (indicated by squares) and in fig. 3 the $\overline{BH}$-curve in dir3 is given with 50 Am in dir2 .One sees that the influence of a lateral field is much higher for dir3 than for dir 2, and that at higher H-values (i.e. much higher than the lateral field applied) the curves with lateral field join again the curves without lateral field.

In fig. 1 a field of $\overline{Hx}$ = 50 Am and $\overline{Hy}$ = 200 Am is applied, resulting in $\overline{Bx}$ = .2622 T and $\overline{By}$ = .0652 T. Solid Fe would have given resp. .2745 T and 1.0980 T.

3. Detector model

A display of the detector model is given in fig. 4. The beam axes coincide with the z-axes. In fig. 5 an xy-cut is shown with part of the grid. The used dimensions are given in section 6. As approximation only two different BH-curves were used, (2) for the xy-plane and (4) for the z-direction.

In fig. 6 the contours of |B| are given in a plane through the beam axes and a toroid coil. Fig. 7 and 8 are similar as 6 but with different upper bounds. Fig. 9 gives the direction of the field in the same plane.

One can see that the return flux of the solenoid is mainly passing through the support bars (70% at center) of the tile calorimeter. The tile calorimeter takes 25% and the front plate 2 %.

In fig. 10 |B| is given along lines (17 in total, see fig. 5) parallel with the beam-axes and passing through the center of the holes in the support bars, i.e. the place where the PM's are located. The field strength is everywhere below 6 gauss, except if one approaches the ends with a distance of the order of the gap size. Fig. 14 shows the contours of |B| in the PM-cavities in a plane perpendicular to the beam axes going through the center of the detector, i.e. where the field is maximal.

In fig. 11, 12 and 13 one sees |B| along lines parallel with the beam axes going resp. through the top, bottom and walls of the support structure.

The increase in the field near the edges of the support is mainly in the phi direction and induced by the toroid. The two peaks at z = +/- 3m in fig.12 are caused by the bottleneck formed by the gaps between forward and barrel tile calorimeter. The forward-backward asymmetries are caused by the solenoidal field.

In fig. 15 and 16 the H_z and H_{phi} components in the tile calorimeter are given. From these figures one can determine that $H_z < 300$ Am, and $H_{phi} < 50$ Am. This means that the local BH-curves of the tile calorimeter do not deviate much from the O and [] curves of fig. 2 and 3 and that the error made by using only two BH-curves is small.

In this calculation only one tile size of 100 mm was used. In order to estimate the effect of this neglect on the field strength in the PM-cavities, the calculation was repeated assuming the tilecal was laminated with packing factor .76, i.e. BH-curve (2) for the xy-plane and $\mu_r = 1/(1-.76)$ in the beam direction. The result for the air gaps is shown in fig. 17. The max. field increased from 6 to 26 gauss. This is an upper bound for the field in the PM-cavities.

The field inside the tiles can be estimated from H_z and H_{phi} given in fig. 15 and 16:

$B_z = 18/4 \times \mu_0 \times H_z$ and $B_{phi} = \mu_0 \times H_{phi}$, which results in a maximum value of 17 gauss in the beam-direction closest to the center of the detector. In the laminated case this value was 80 gauss, which is an upper limit.

4. Conclusions

From the above calculation, with the dimensions of section 6, it seems unlikely that the magnetic field inside the cavities of the support structure will exceed the value of 10 gauss, and the field inside the scintillating tiles the value of 20 gauss.

5. Possible improvements

The above calculation was done to estimate the magnetic field upper limits in the PM-cavities and inside the tiles. For a more precise determination of the field a more complete BH-matrix should be applied. Such a matrix could be calculated as above on a test-cell in a reasonable time.

A method immediately applicable is to create regions with different BH-curves, which by iteration could be adapted to the local H-field.

Much better would be if the manufacturer of the used program (TOSCA from Vector-Fields ltd.) would allow the user to assign the mu-value to each element individually in the mu-iteration. So far negotiations with Vector-Fields were not successful.
In addition it is possible, by using symmetry , to reduce the model by a factor 4 , but also here the cooperation of the manufacturer is necessary.
Another possible refinement is the inclusion of the forward toroids.

6. Dimensions

all lengths in m

Support bars:

thickness outer layer: .1
thickness inner layer: .11
radial walls: .18 x .035
rmin, rmax : 3.81 , 4.2
length in beam dir: 12.292

Tile calorimeter:

endplate thickness: .02
front plate thickness: .01
length barrel tilecal in z-direction: 5.894
length extended barrel tilecal in z-direction: 2.699
gap size between barrel and ext. barrel tilecal: .5
rmin, rmax tilecal: 2.25 3.81

toroid:

8 x conductor .45 x .352
inner cond at 5.315 from beam axes
outer cond at 9.145 from beam axes
length in z-direction 25.5
radii of bent parts 1
current 8 x 3 MAmp

solenoid:

length 6.3
inner radius 1.23
outer radius 1.2428
current 10.6 MAmp

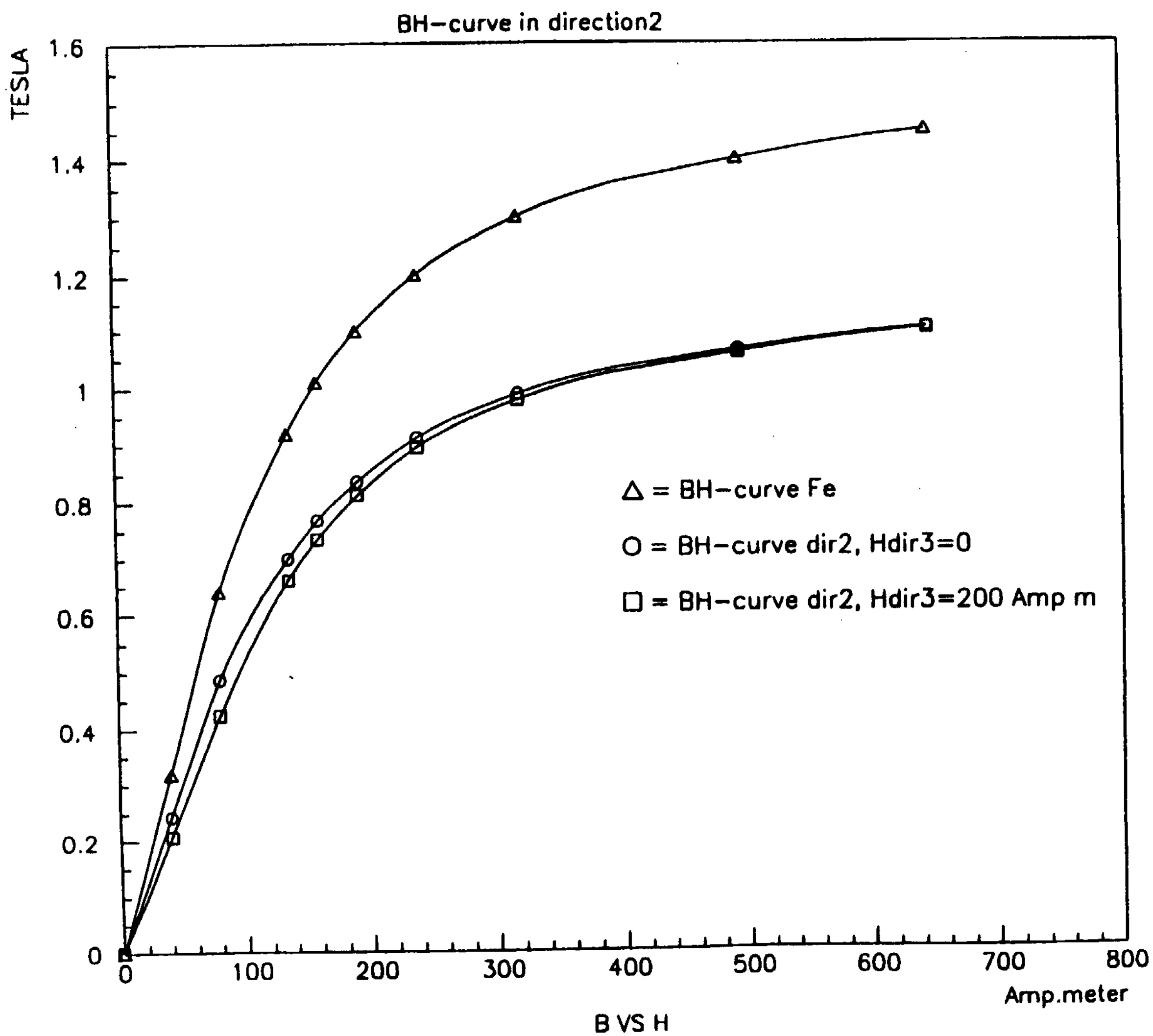

Fig.2 : BH-curve in direction 2

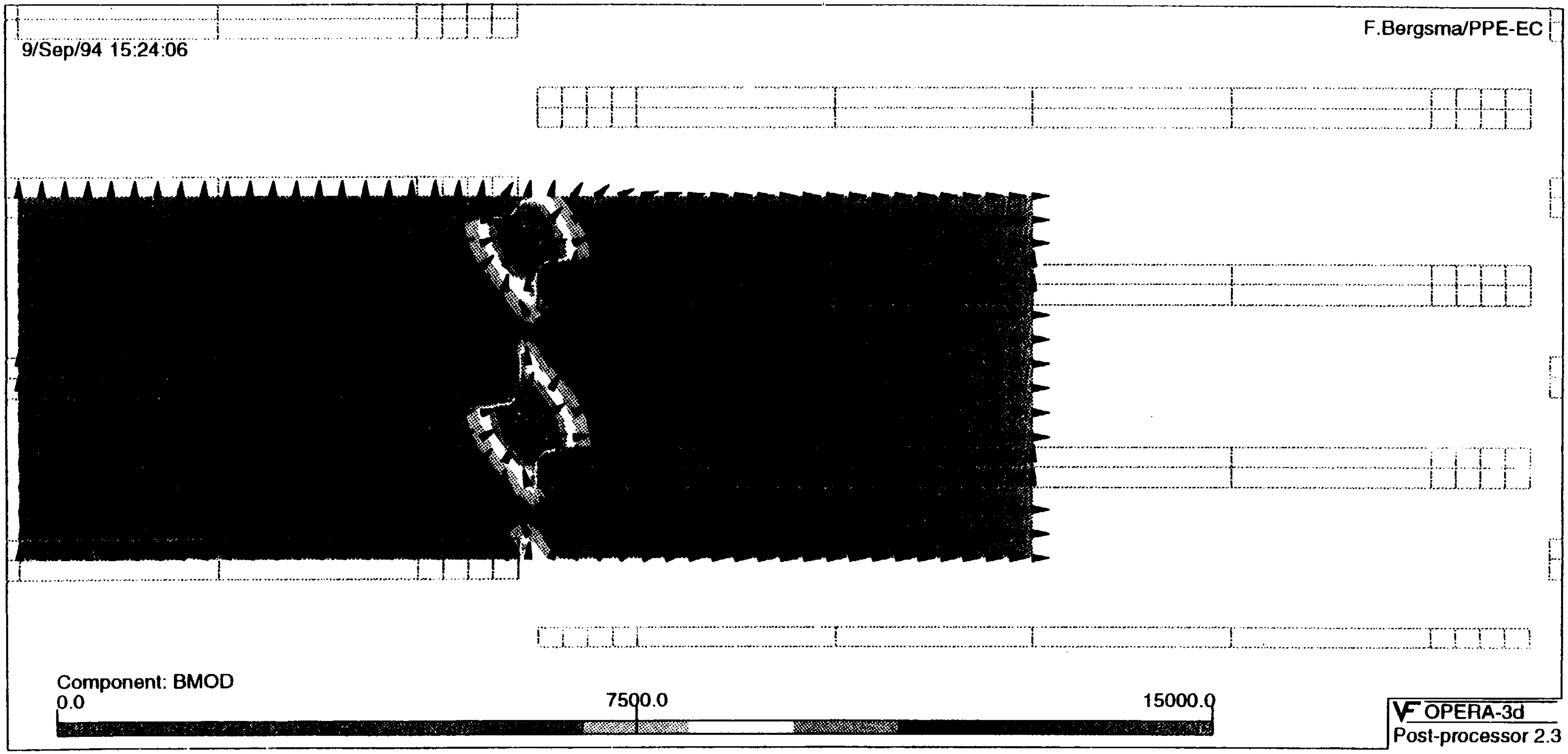

Fig.1 : Contours of the absolute value of the magnetic field in the tile calorimeter at $H_{dir1} = 0$, $H_{dir2} = 50$ Amp m, $H_{dir3} = 200$ Amp m. The scale is in gauss.

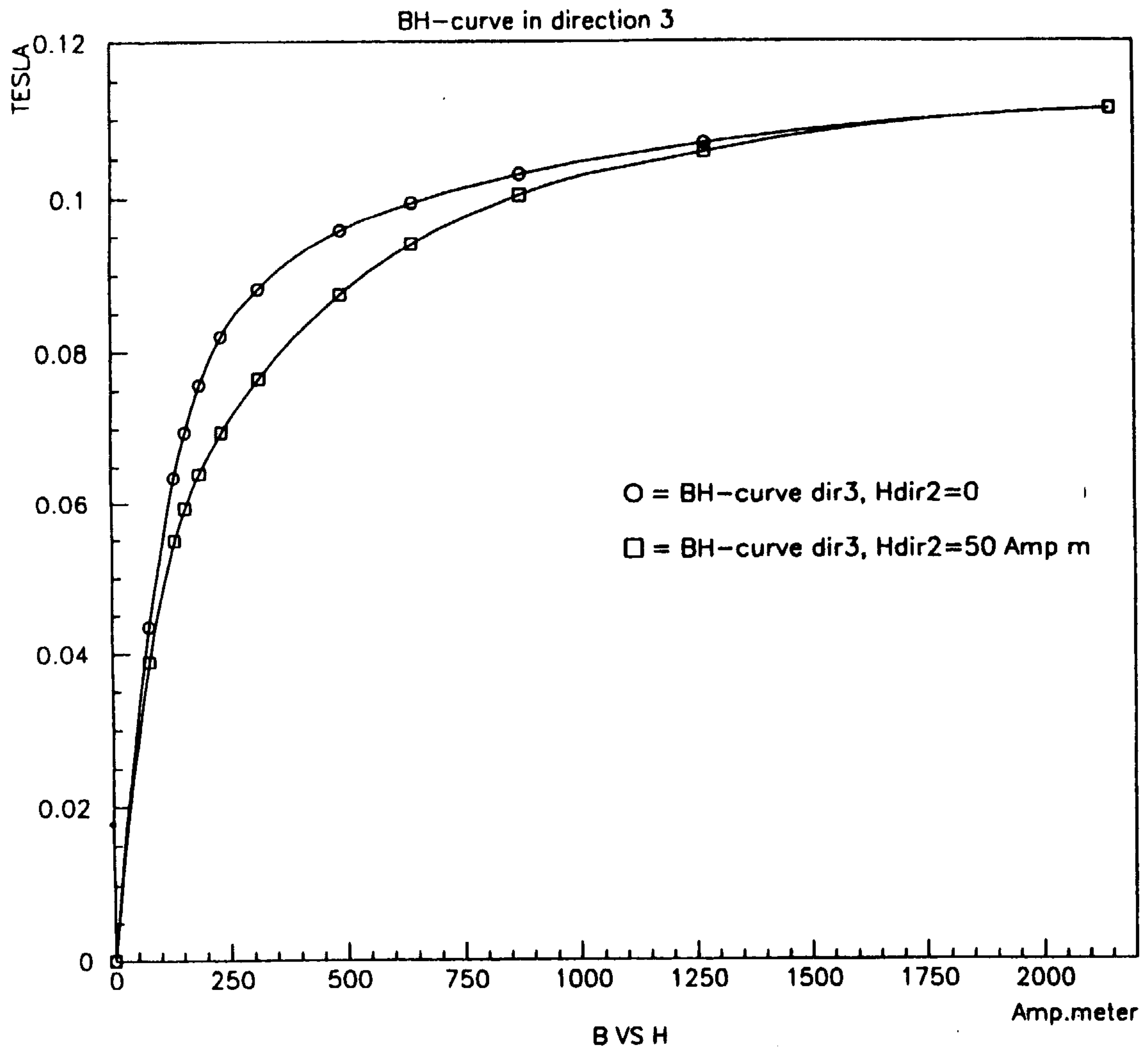

Fig.3 : BH-curve in direction 3

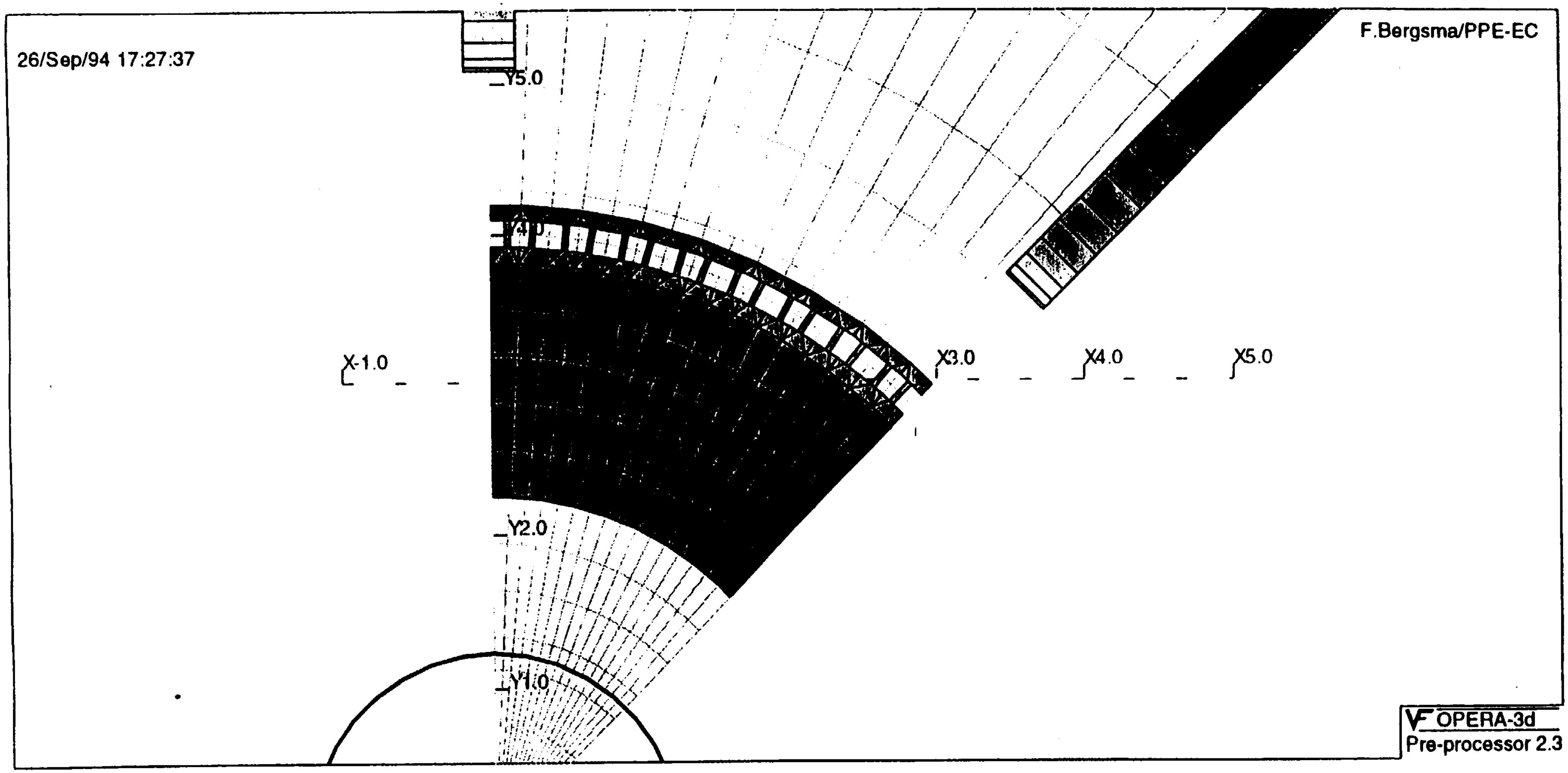

Fig.5 : xy-cut (perpendicular to beam-axes) of the detector model

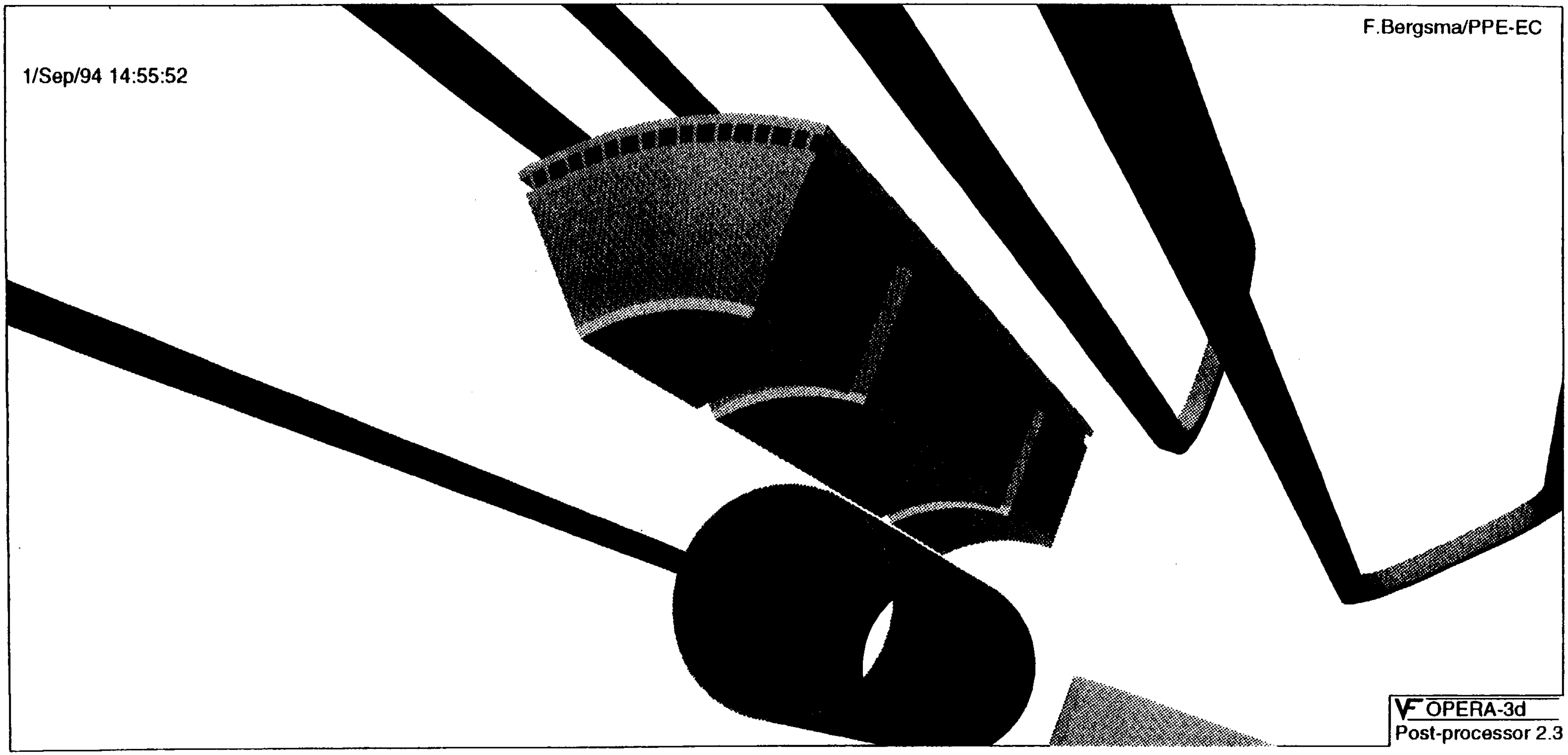

Fig.4 : perspective view of the detector model

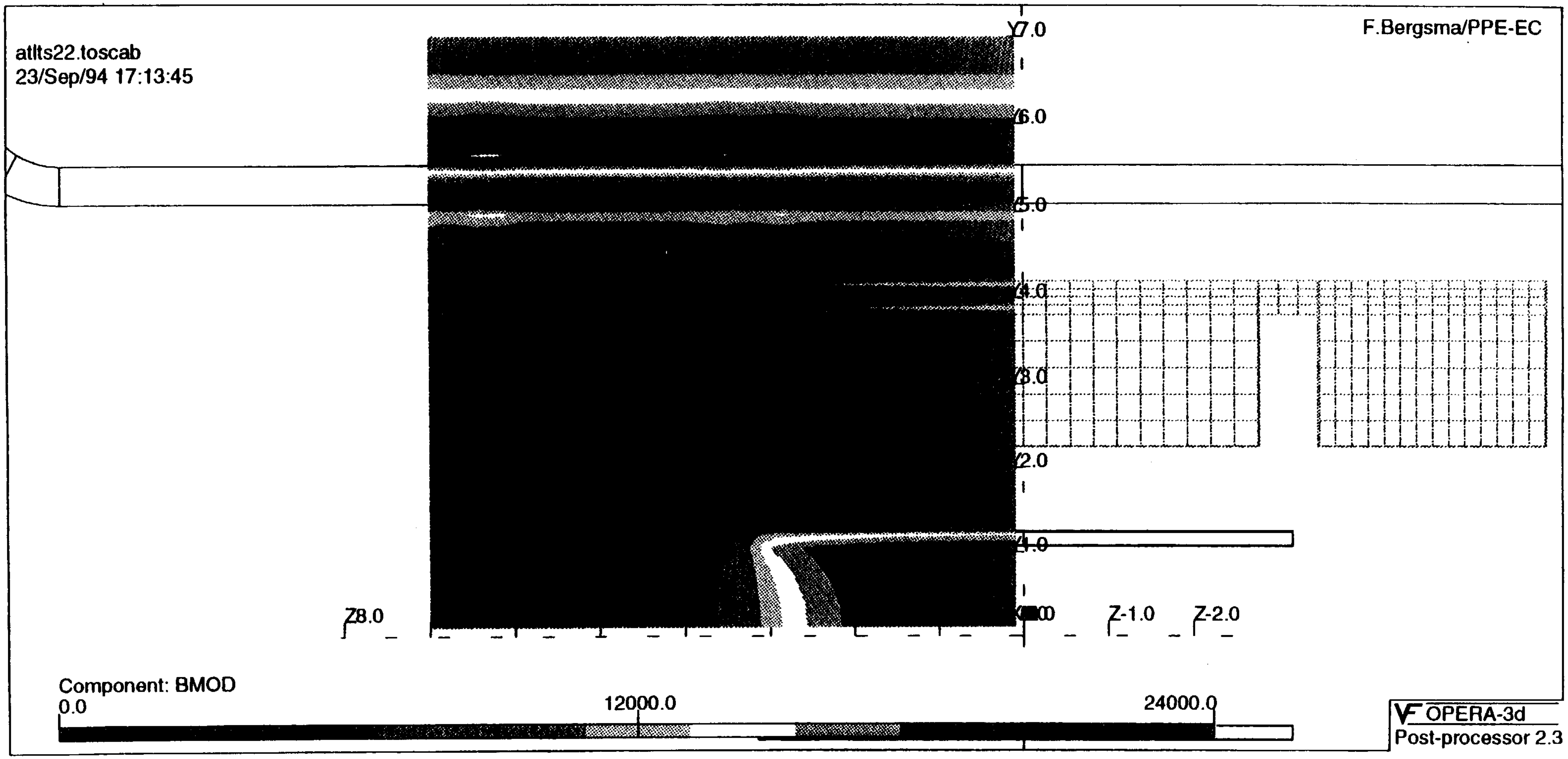

Fig.6 : Contours of the absolute value of the magnetic field in a plane through the beam axes and one of the toroid coils. The scale runs from 0 to 24000 gauss.

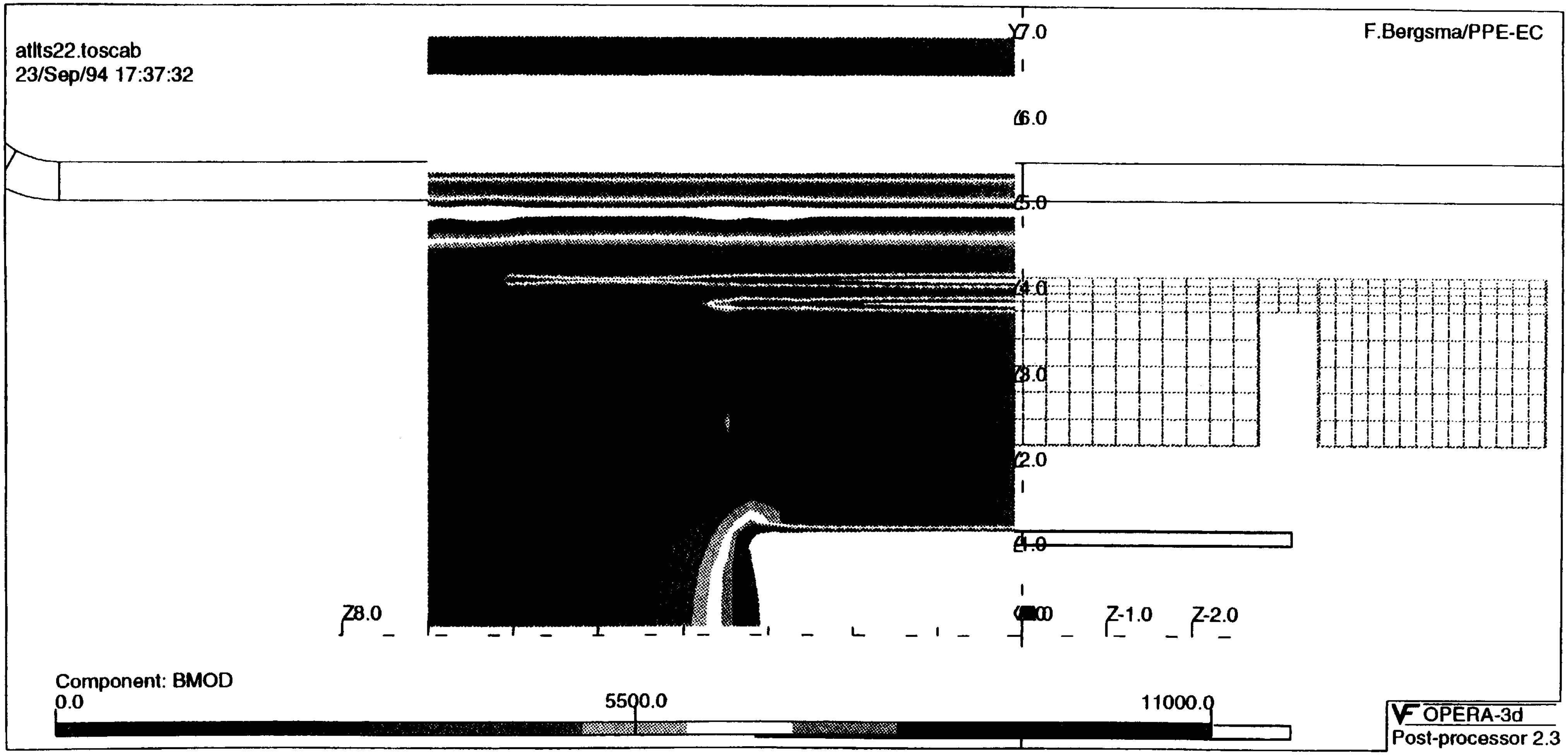

Fig.7 : Contours of the absolute value of the magnetic field in a plane through the beam axes and one of the toroid coils. The scale runs from 0 to 11000 gauss.

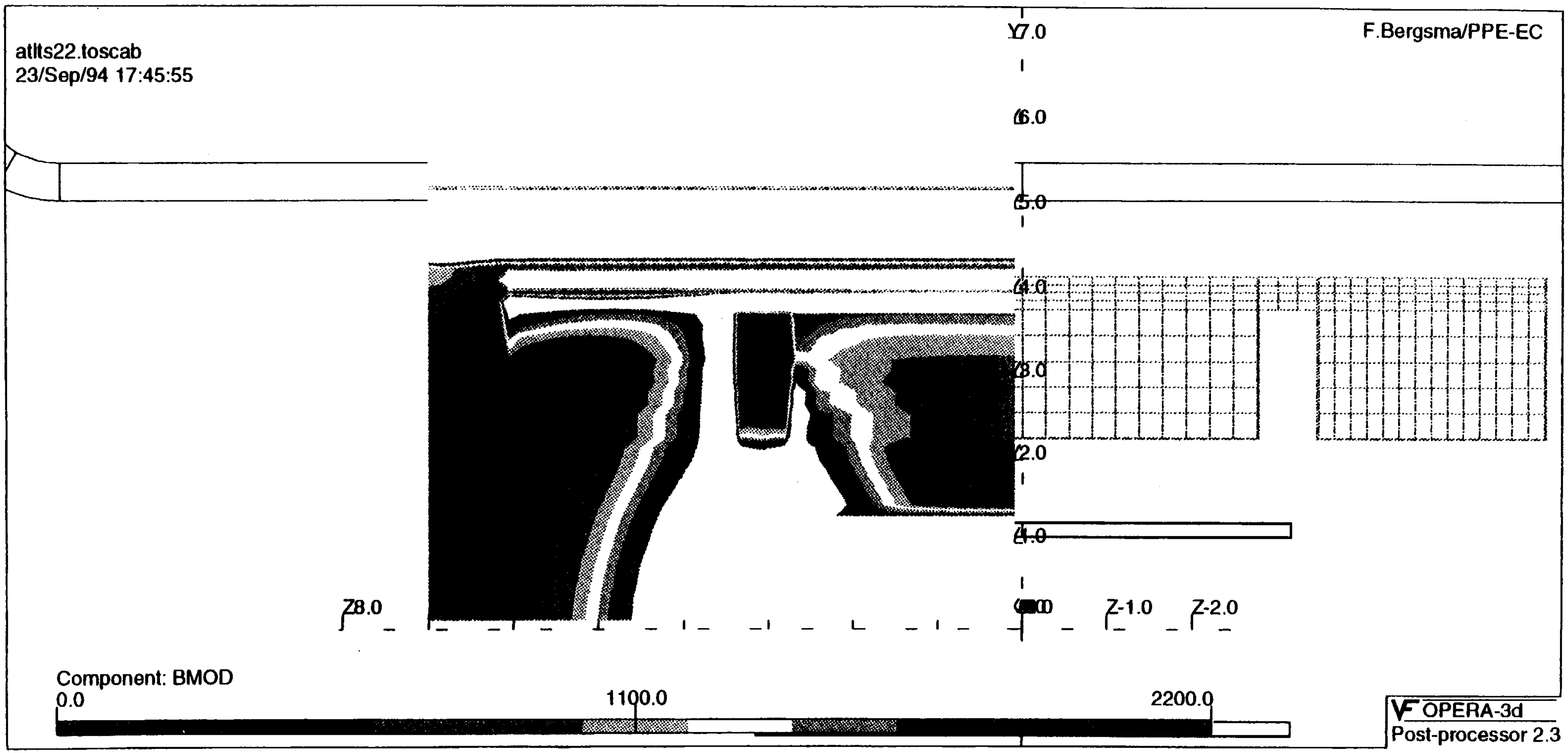

Fig.8 : Contours of the absolute value of the magnetic field in a plane through the beam axes and one of the toroid coils. The scale runs from 0 to 2200 gauss.

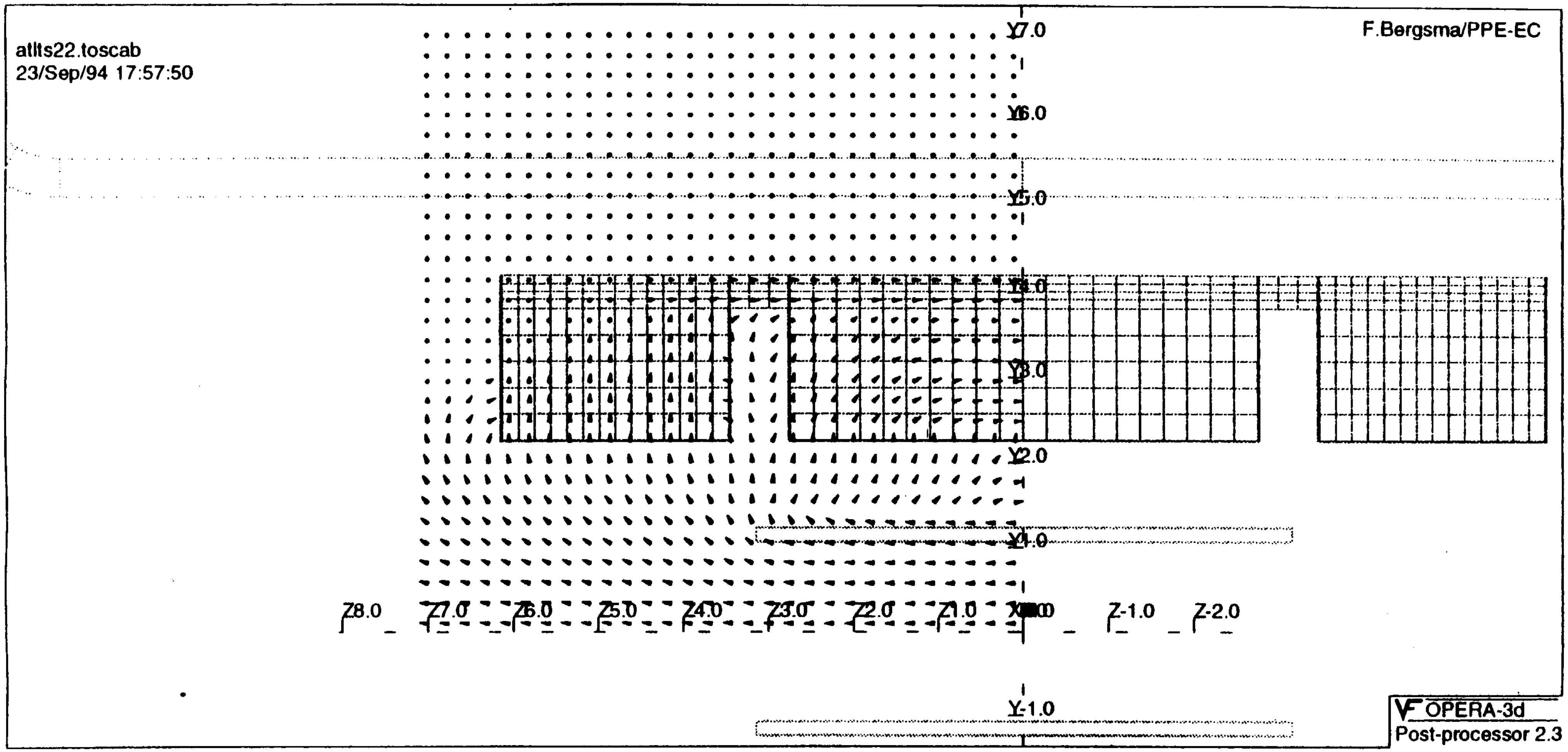

Fig.9 : Direction of the magnetic field in a plane through the beam axes and one of the toroid coils.

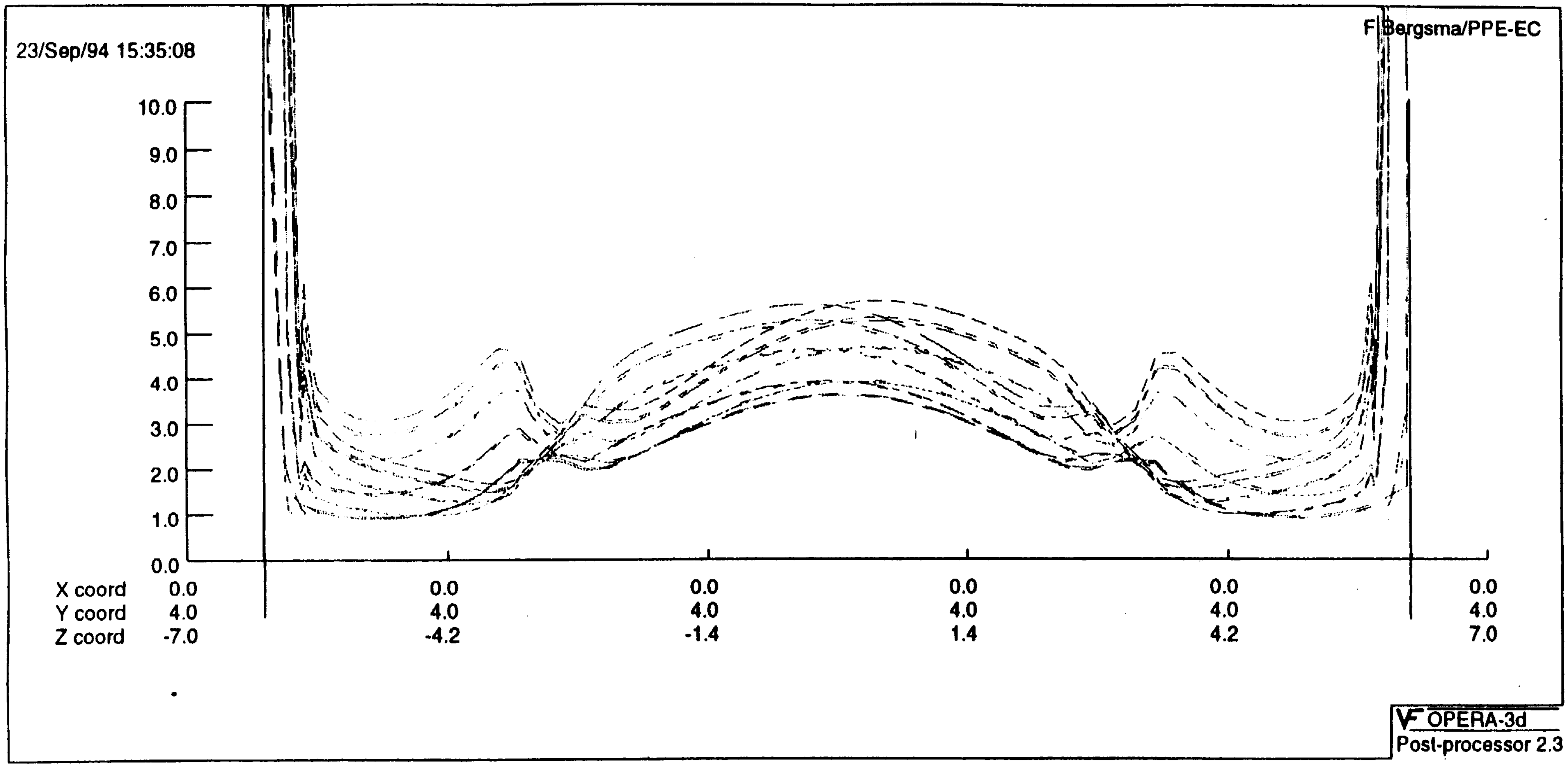

Fig.10 : Absolute value of the magnetic field along 17 lines parallel to the z-axes passing through the center of the air gaps in the support structure. The vertical lines indicate the limits of the support.

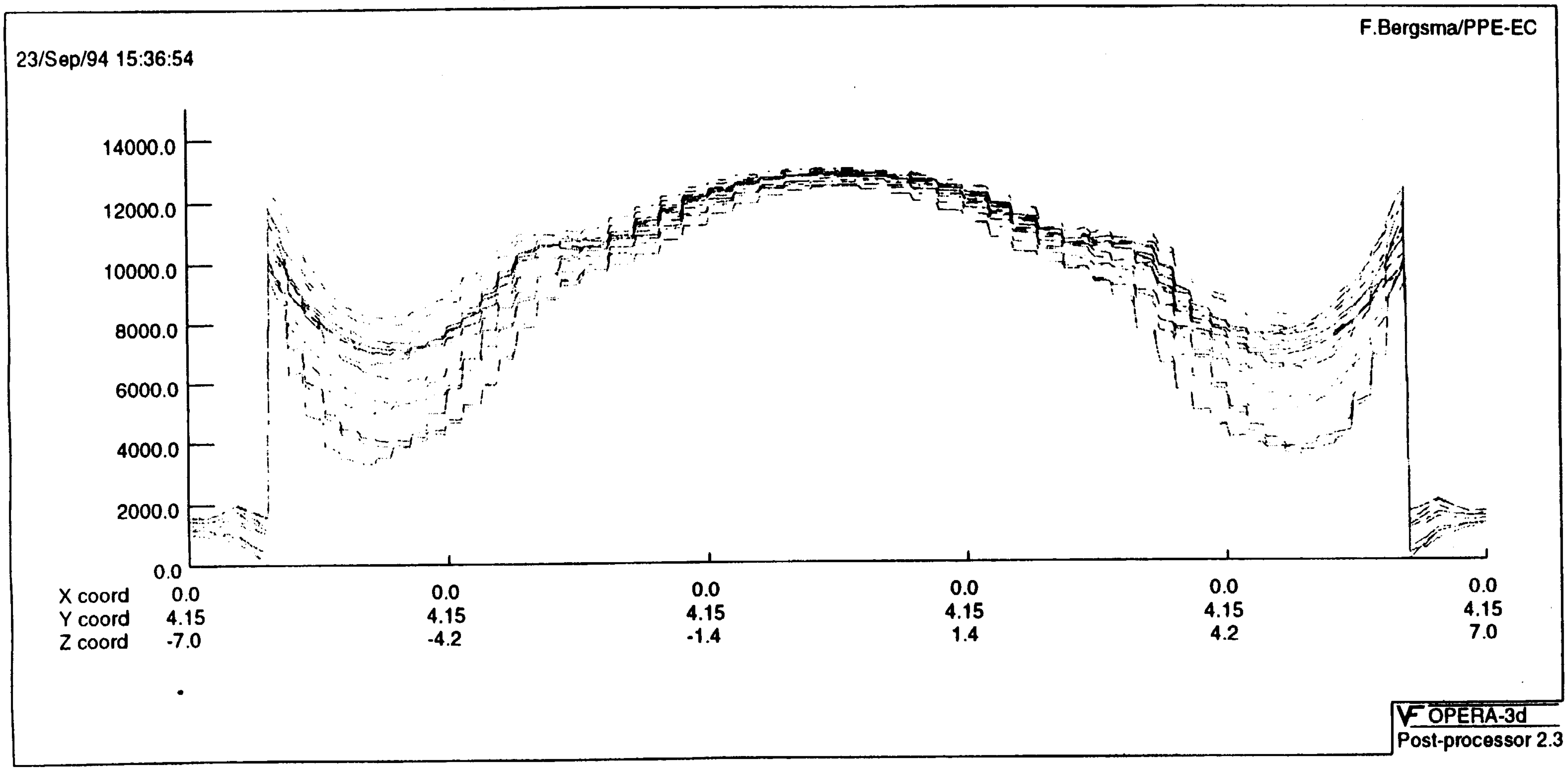

Fig.11 : Absolute value of the magnetic field along 17 lines parallel to the z-axes passing through the outer layer of iron of the support structure.

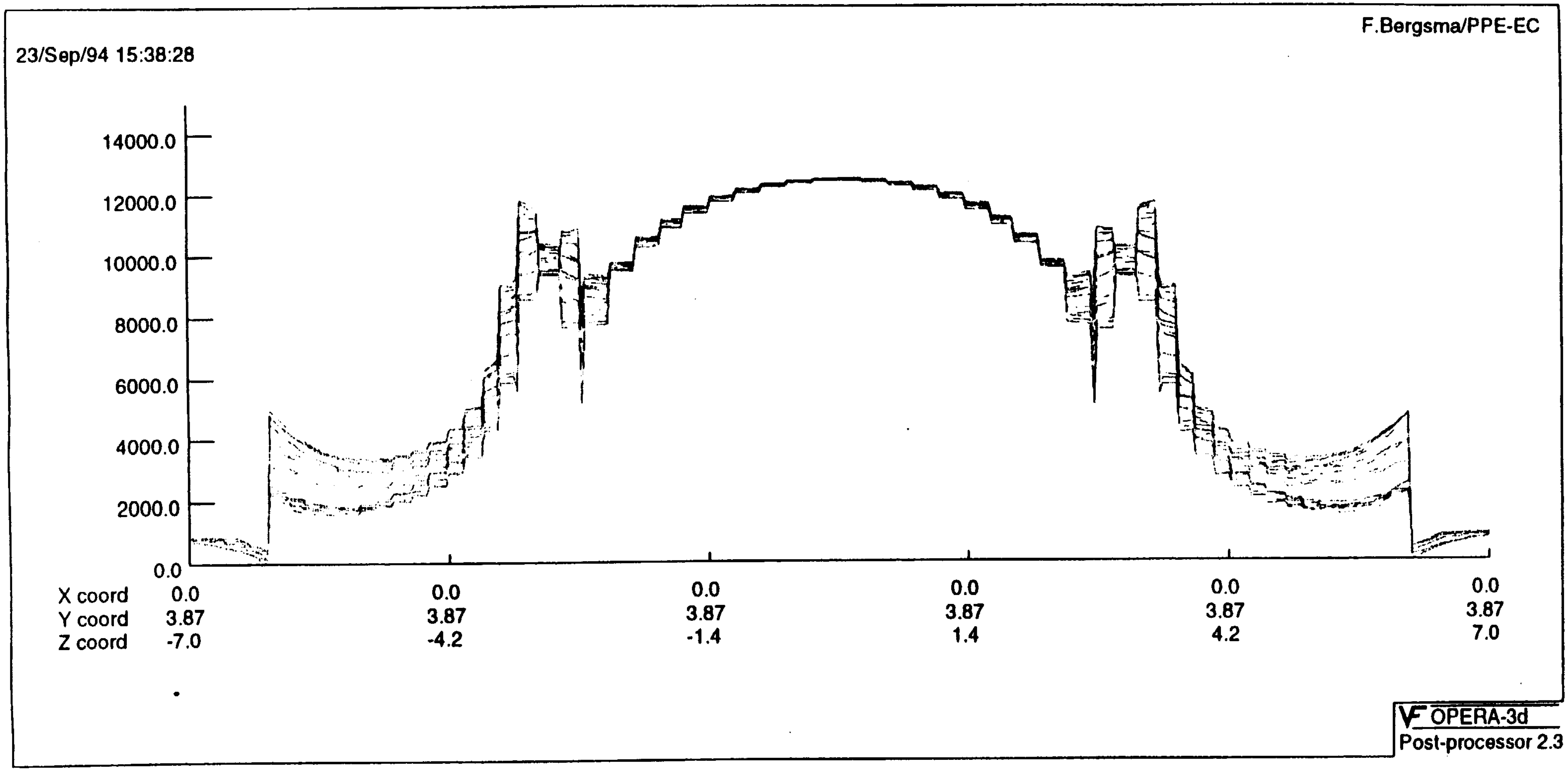

Fig.12 : Absolute value of the magnetic field along 17 lines parallel to the z-axes passing through the inner layer of iron of the support structure.

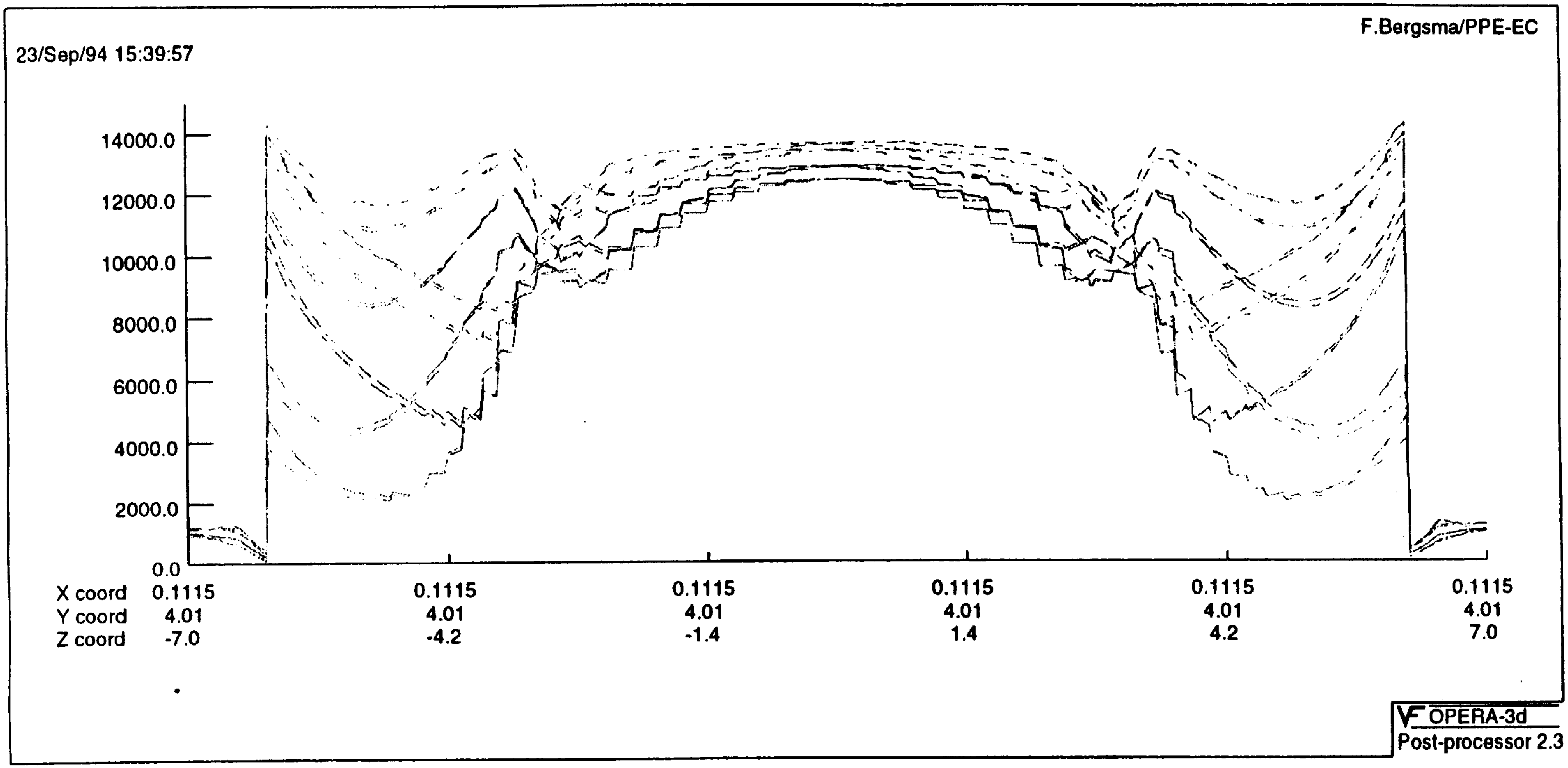

Fig.13 : Absolute value of the magnetic field along 16 lines parallel to the z-axes passing through the center of the radial iron walls of the support structure.

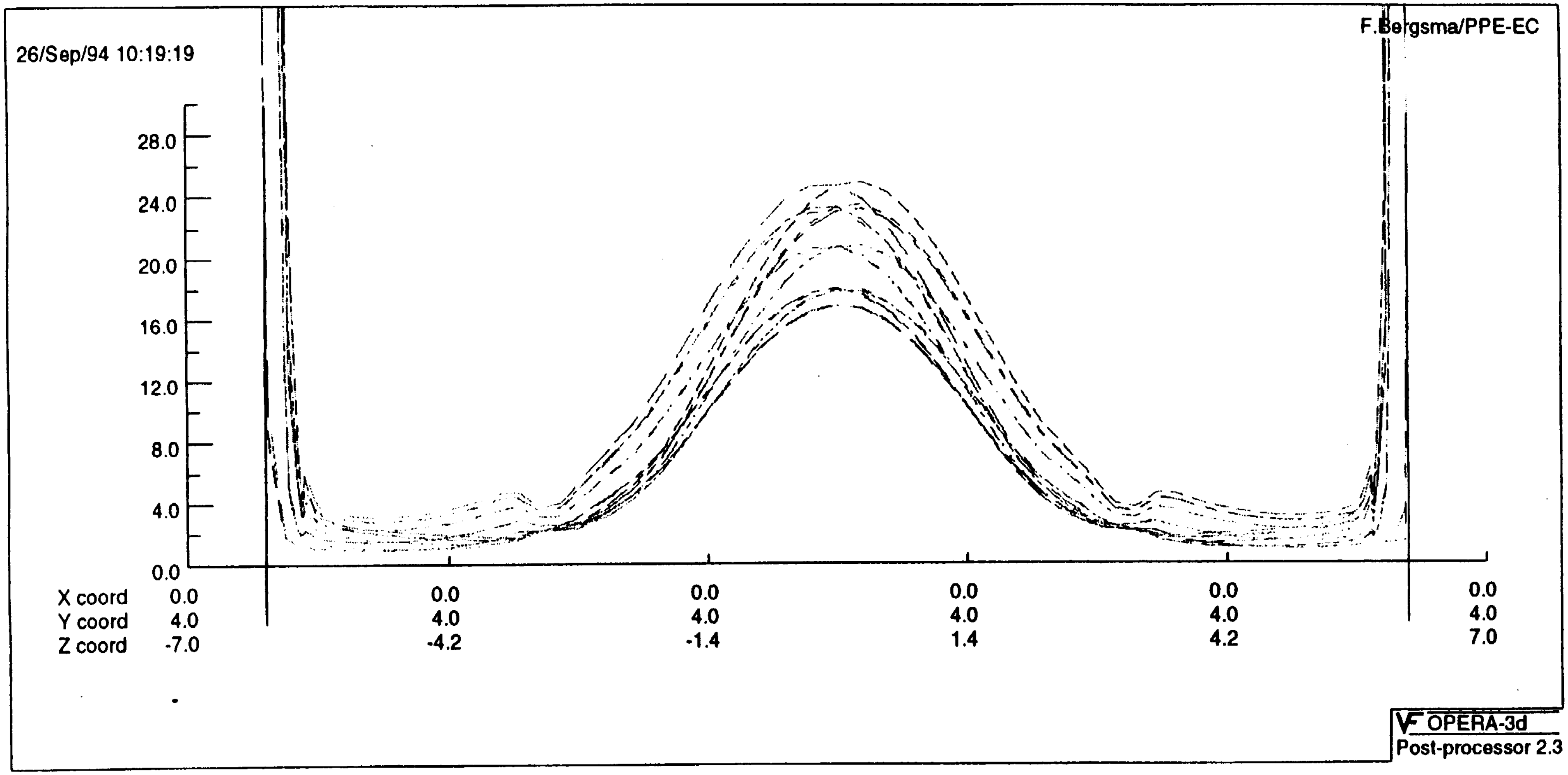

Fig.17 : Absolute value of the magnetic field along 17 lines parallel to the z-axes passing through the center of the air gaps in the support structure with the tile calorimeter treated as laminated with packing factor .76 . The vertical lines indicate the limits of the support.

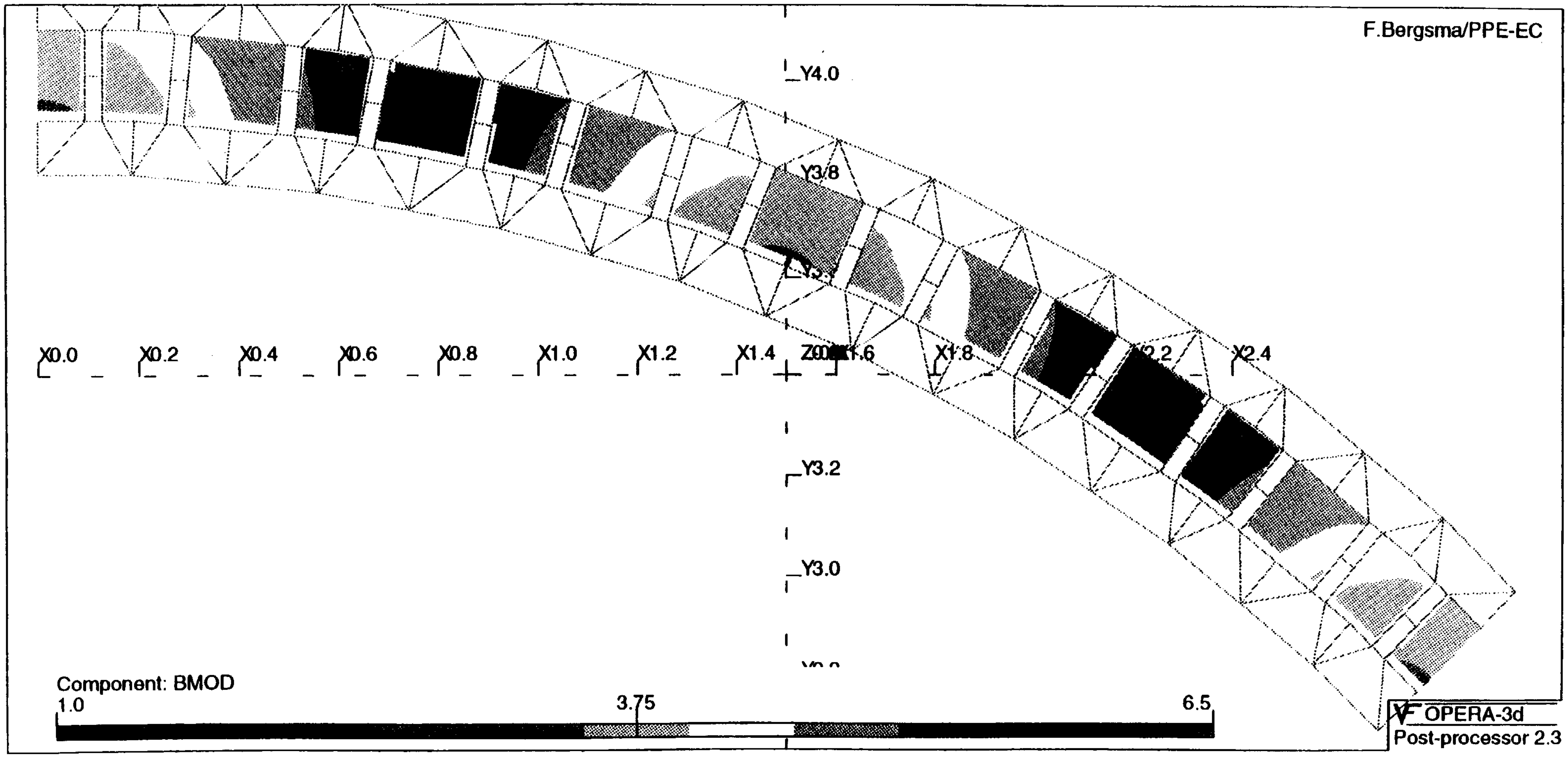

Fig.14 : Contours of the absolute value of the magnetic field in the PM-cavities in a plane perpendicular to the beam axes through the center of the detector.

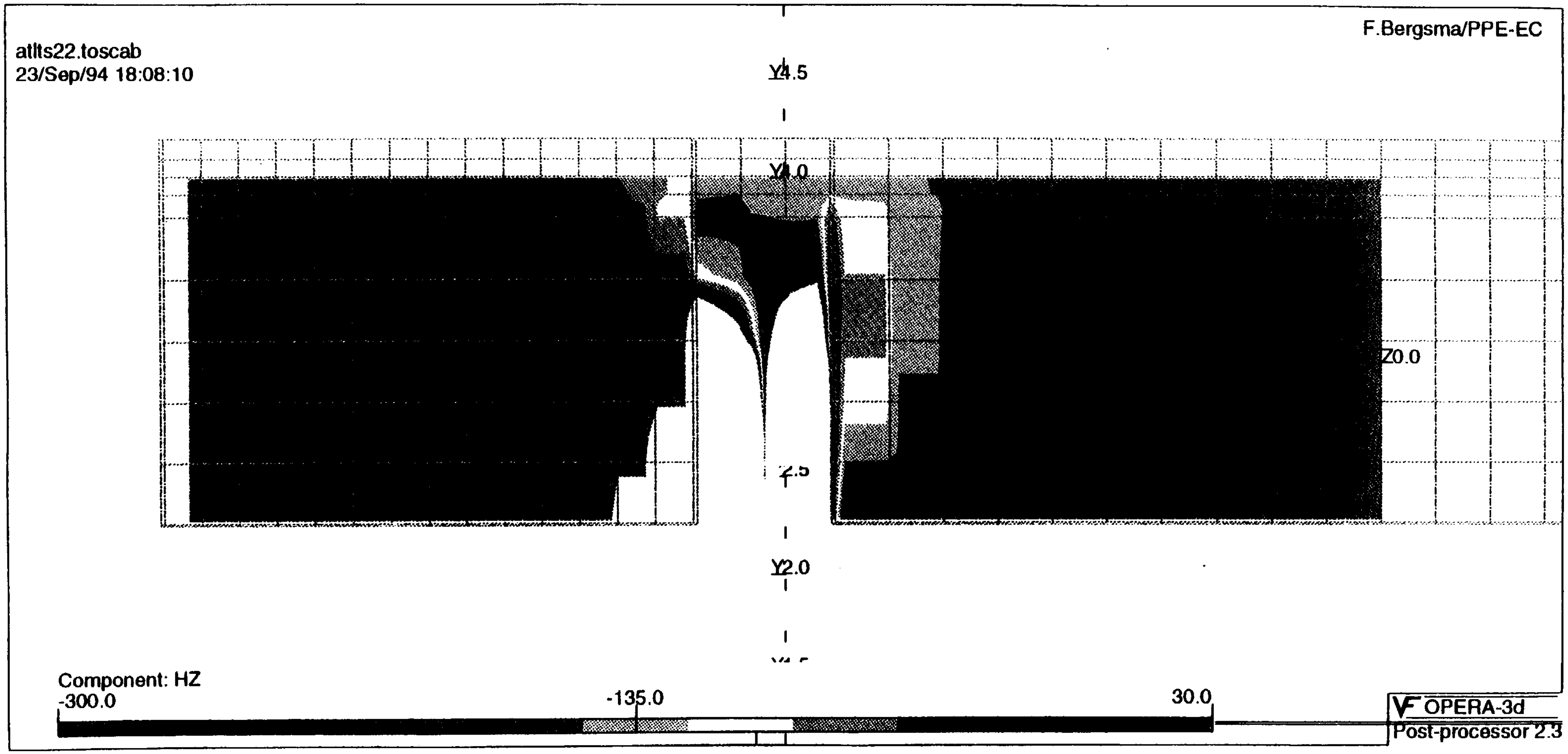

Fig.15 : Contours of the dir3-component of H in the tile calorimeter in a plane through the beam-axes and one of the toroid coils.

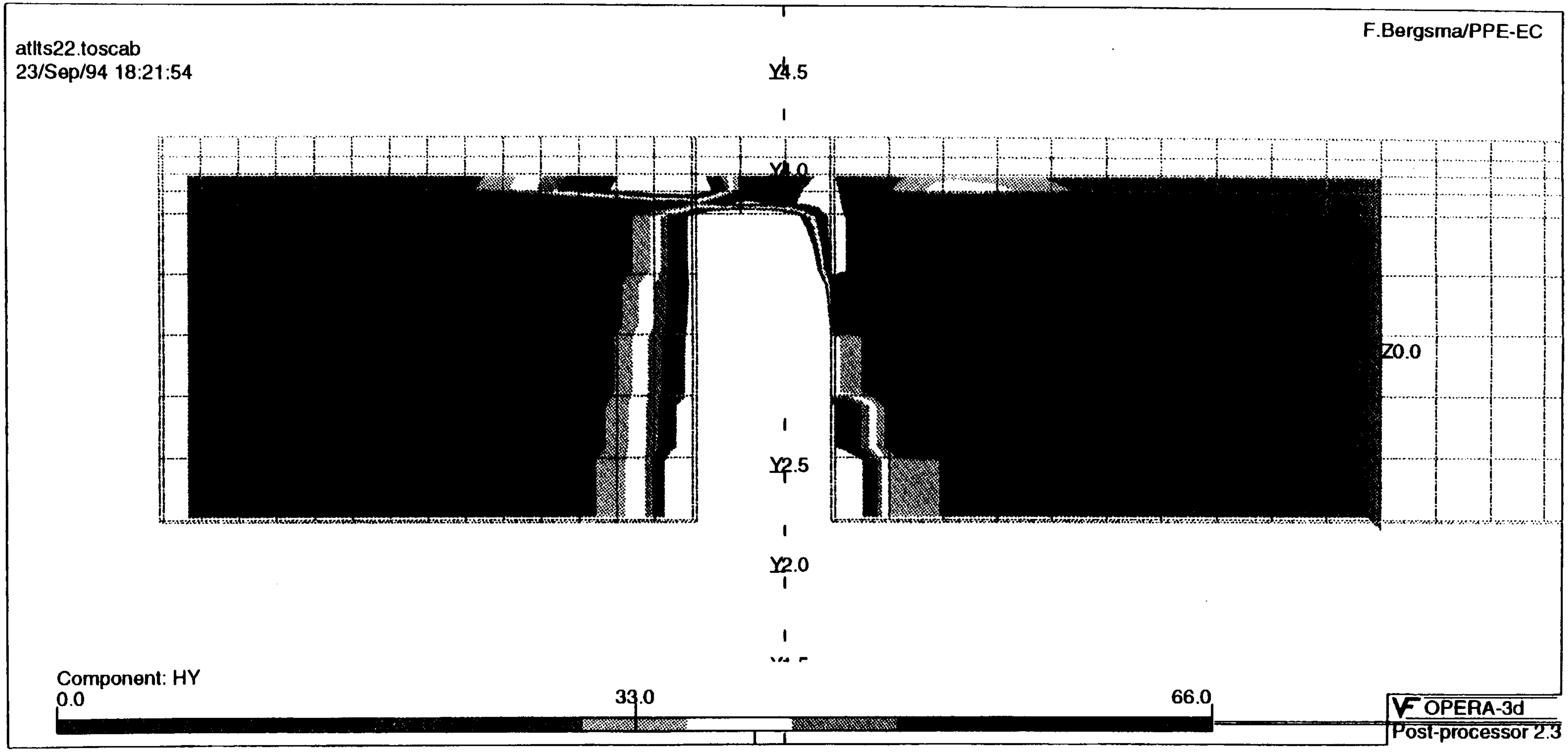

Fig.16 : Contours of the dir2-component of H in the tile calorimeter in a plane through the beam-axes and one of the toroid coils.